Thermal conductivity of YBCO(123) and YBCO(211) mixed crystals prepared by MMTG

M. Ikebe, H. Fujishiro, T. Naito, K. Noto, S. Kohayashi* and S. Yoshizawa*

Department of Materials Science and Technology, Faculty of Engineering, Iwate University, 4-3-5, Ueda, Morioka 020, Japan
*Central Research Laboratory, Dowa Mining Co. Ltd, Tobukicho, Hachioji, Tokyo 192, Japan

Received 17 May 1993; revised 7 July 1993

The *a-b* plane and *c*-axis thermal conductivity of $YBa_2Cu_3O_{7-X}$ bulk superconducting crystals prepared by modified melt texture growth (MMTG) was studied. The crystals contained finely dispersed Y_2BaCuO_5 particles which were expected to form pinning centres. The conductivity data were analysed based on a proposed model for the mixed crystals using the conductivity of polycrystalline Y_2BaCuO_5. The analyses indicate that Y_2BaCuO_5 particles reduce the conductivity of MMTG crystals in the *a-b* plane but hardly influence the conductivity along the *c*-axis.

Keywords: YBCO; material properties; thermal conductivity

Melt growth processed Y-Ba-Cu-O superconductors exhibit a high critical current density J_c at the boiling point of liquid nitrogen and it is possible to fabricate large bulk crystals. These crystals are expected to have practical applications in the near future, such as in power current leads and magnetic shieldings. A common feature of crystals obtained through the various melt growth processes for $YBa_2Cu_3O_{7-X}$, e.g. quench and melt growth (QMG)[1], melt texture growth (MTG)[2], etc. is that fine Y_2BaCuO_5 (211) phase particles are dispersed in the $YBa_2Cu_3O_{7-X}$ (123) matrix phase. The existence of the (211) impurity phase in an appropriate form and quantity is assumed to be effective in increasing the pinning force and in preventing the matrix crystal from cracking.

The thermal conductivity κ of the oxide superconductors is a physically important quantity which reflects the strength of the interaction between phonons and charge carriers. It is also a very important measure of the quality of a crystal, as it reflects phonon and defect interaction in solids. For power current lead design, κ is a fundamental quantity needed to calculate the heat intrusion and the necessary cooling power. Several thermal conductivity measurements have been reported for $YBa_2Cu_3O_{7-X}$ polycrystals[3–5] and single crystals[6–8]. The thermal conductivity of melt growth processed crystals, however, has hardly been reported at all, probably because the mixed structure of the (123) and (211) phases is regarded as inappropriate for physical investigations. Yamamoto *et al.*[9] reported the themal conductivity of $YBa_2Cu_3O_{7-X}$ samples with and without Ag doping, fabricated by the melt powdering melt growth (MPMG) method from a Y_2O_3:$BaCO_3$:CuO = 1:4:6 melt. Their measurements were confined to a relatively narrow temperature range and the discussion on the effect of the impurity phase was brief.

In this paper, we report the thermal conductivity of $YBa_2Cu_3O_{7-X}$ crystals prepared by the modified melt texture growth (MMTG) method and discuss the effect of the (211) impurity phase, based on a proposed model. The MMTG method is one of the melt growth methods for Y-Ba-Cu-O crystals. The J_c of the obtained single grain crystal was found to be larger than 10^4 A cm^{-2} at 77 K, 0 T[10], which was comparable to good crystals prepared by other methods. The magnetic shielding effect and the magnetic relaxation of the present crystals have been reported already[11].

Using the MMTG method, the (211) phase can be finely dispersed in the (123) matrix and the amount of the (211) phase can be controlled by adjusting the ratio of the starting mixture of Y_2O_3 and BaCuO. Since no crucible is used, the MMTG method has an advantage of being almost free from impurity atom contamination for the grown crystals.

Experimental details

Sample preparation

A raw powder of $BaCO_3$ and CuO mixed with a mole ratio of 1:1 was calcined at 850°C for 30 h in air. The calcined material was pulverized, and Y_2O_3 and CuO powders were added to the pulverized powder. In this work, two types of powder mixture were used, corresponding to weight ratios of (123):(211) = 1:0.4 for sample 1 (S1) and 1:0.3 for sample 2 (S2), respectively.

0011-2275/94/010057-05

Platinum (Pt) powder was added at a level of 0.5 at% in order to make the (211) phase disperse finely. These powders were mixed and uniaxially pressed up to 2000 kg cm^{-2} to form a pellet. The MMTG heat pattern is schematically illustrated in *Figure 1*. After heating at 1100°C for 30 min in air, the pellet was quenched to 1000°C and cooled slowly down to 940°C at the rate of 1°C h^{-1} using a unidirectional growth technique involving controlling the temperature gradient in the sample. Finally, the sample was annealed at 600°C for 200 h in an oxygen atmosphere.

The (211) polycrystals were prepared via a solid state reaction method in the following way. A mixed powder of Y_2O_3, $BaCO_3$ and CuO with a mole ratio of 1:1:1 was calcined at 900°C for 15 h in air. After pulverizing the calcined materials, they were pressed into pellets and were sintered at 950–1100°C for 15 h in air.

Measurement technique

The crystal axis of the grown material was determined by X-ray diffraction using Cu Kα radiation. The two S1 samples used for the measurements were cut with a diamond saw to a size of 4.2 × 2.8 × 9.0 mm^3 and 3.7 × 2.5 × 7.0 mm^3, respectively. The latter specimen was 7.0 mm in length along the *c*-axis and was used for the *c*-axis conductivity measurement. The two S2 samples were cut to a size of 3.0 × 2.8 × 12.0 mm^3 and 2.1 × 1.8 × 1.0 mm^3, respectively. The thermal conductivity was measured by the steady state heat flow method with an automated measuring system of our own making, in which a closed cycle helium refrigerator system was used as the cryostat. One end of the sample was soldered to the cold head of the cryostat and a small chip resistance heater made of a metallic thin film was adhered to the other end of the sample using GE7031 varnish. Au + 0.07 at% Fe–chromel thermocouples (72 μm in diameter) were differentially used to measure the temperature difference. The electrical resistivity was measured by a conventional four-probe method using a closed cycle helium refrigerator. The density of the samples was measured using the Archimedean principle using xylene. Microstructural observations and analyses were performed by a polarized optical microscope and a scanning electron microscope (SEM).

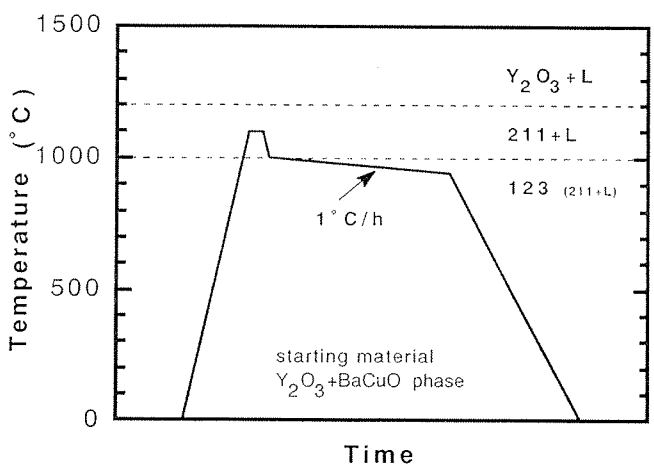

Figure 1 Schematic diagram of heat pattern for MMTG method

Results and discussion

Metallographic observations and electrical resistivity

To investigate the dispersion of the (211) phase particles in the (123) matrix phase, observation by an optical microscope was performed. *Figure 2* shows a polarized optical micrograph of the *a-b* plane of the S1 crystal. Crystal grains of the matrix phase as large as a few millimetres in size were obtained. Although the MMTG method is different from other melt growth methods with respect to the starting phase and the heat pattern, grains of the (123) matrix were still developed. In the figure, the small bright particles can be seen to be finely dispersed. A quantitative wavelength dispersive spectral analysis confirmed that the matrix and the dispersed particles were the (123) phase and the (211) phase, respectively.

The estimated composition ratio of 0.3 for the (211) phase from the optical micrographs seemed to be consistent with the nominal composition ratio of 0.286 (= 0.4/1.4) for the S1 sample. As the Pt content was low, the size of the (211) phase, which was less than 10 μm, was not uniform in the matrix phase. For the sample surface perpendicular to the *a-b* plane, a similar dispersion of the fine (211) particles was also observed, which indicated that the (211) particle dispersion occurred almost independently of the crystal axes of the (123) matrix.

Figure 3 shows the *a-b* plane (ρ_{ab}) and the *c*-axis (ρ_c) electrical resistivity *versus* temperature *T* of samples S1 and S2. There was a significant difference in the ρ_{ab} values of S1 and S2: ρ_{ab} of S2 being about a factor of 10 larger ($\approx$ 100 K) than that of S1. This result suggests that the best growth condition was not applied to the S2 crystal and that various defects were introduced into the S2 crystal.

The ρ_c of S2 is also about twice as large as that of S1 at 100 K. The anisotropy ratio of the resistivity ρ_c/ρ_{ab} is $\approx$ 90 for S1 and $\approx$ 15 for S2 at 100 K. Although ρ_c of

Figure 2 Polarized optical micrograph of *a-b* plane surface of grown crystal

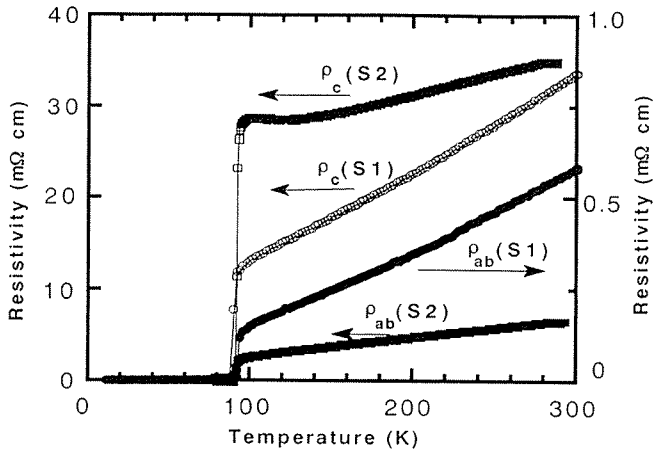

Figure 3 Temperature dependence of electrical resistivity of mixed crystals, S1 and S2 in the *a-b* plane (ρ_{ab}) and along *c*-axis (ρ_c)

$YBa_2Cu_3O_{7-X}$ shows both metallic[12,13] and semiconductive [14,15] behaviour, depending on the samples, the present S1 and S2 values showed metallic behaviour. However, samples S1 and S2 are not perfect single crystals and it is not clear whether the metallic behaviour of ρ_c of the present samples reflects an intrinsic property of $YBa_2Cu_3O_{7-X}$ or whether it originates from crystalline axis misalignment and/or the mixed nature of the (123) and (211) phases. The superconducting transition temperature T_c determined from the resistivity measurement was 90 K for both the S1 and S2 samples.

Thermal conductivity

Figure 4 shows the temperature dependence of the *a-b* plane thermal conductivity κ_{ab} of S1 and S2 and the *c*-axis thermal conductivity κ_c of S1. With decreasing temperature, κ_{ab} for S1 slightly increases between 200 K and T_c and shows a significant upturn near T_c. The maximum of κ_{ab} for S1 occurs around 55 K and then κ_{ab} decreases steeply with further decreases in temperature.

The temperature dependence of κ_{ab} bears a qualitative resemblance to that of the thermal conductivity of sintered $YBa_2Cu_3O_{7-X}$ polycrystals[3]. The absolute values of κ_{ab} are larger than those of the sintered samples and are nearly the same as the reported values for pure single crystals[16]. κ_c for S1, which is almost constant above T_c, shows a discernible upturn from T_c and decreases with decreasing temperatures. The observed anisotropy ratio, κ_{ab}/κ_c, of S1 is ≈ 5 and is nearly constant over the whole temperature range.

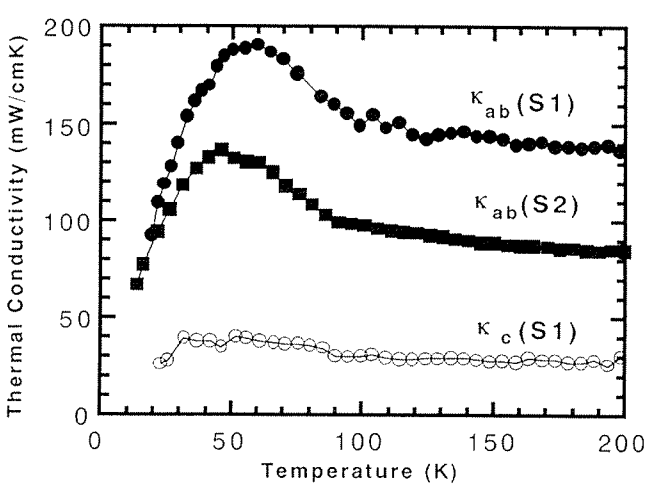

Figure 4 Temperature dependence of observed thermal conductivity in *a-b* plane (κ_{ab}) and *c*-axis (κ_c). κ_c of S2 was not measured because of inappropriate sample shape

As can be seen in *Figure 4*, κ_{ab} of S2 with the nominal (211) composition ratio 0.231 (= 0.3/1.3; by weight) is $\approx 60\%$ of that for S1 with the (211) ratio 0.286. A somewhat similar reduction in the magnitude of the thermal conductivity with decreasing (211) phase content was noted by Buravoi *et al.*[17] for multiphase Y-Ba-Cu-O ceramics. Together with the high value of electrical resistivity ρ_{ab}, the low κ_{ab} value seems to reflect the worse growth conditions in the case of S2. From the resistivity values, the electronic contribution κ^e to the thermal conductivity can be estimated using the Wiedemann–Franz law. Above T_c, the estimated κ^e_{ab} is $\approx 6\%$ of the observed κ_{ab} and κ^e_c is $\approx 0.5\%$ of the observed κ_c for S1, and κ^e_{ab} is $\approx 1\%$ for S2. Thus, the phonon contribution κ^{ph} is much larger in the present specimens. κ_c for S2 was not measured because the sample could not be cut in a suitable shape.

Model analysis of thermal conductivity of mixed crystals

In the present MMTG crystals, a number of (211) fine particles are dispersed in the (123) matrix, as schematically shown in *Figure 5a*. With this arrangement, the heat

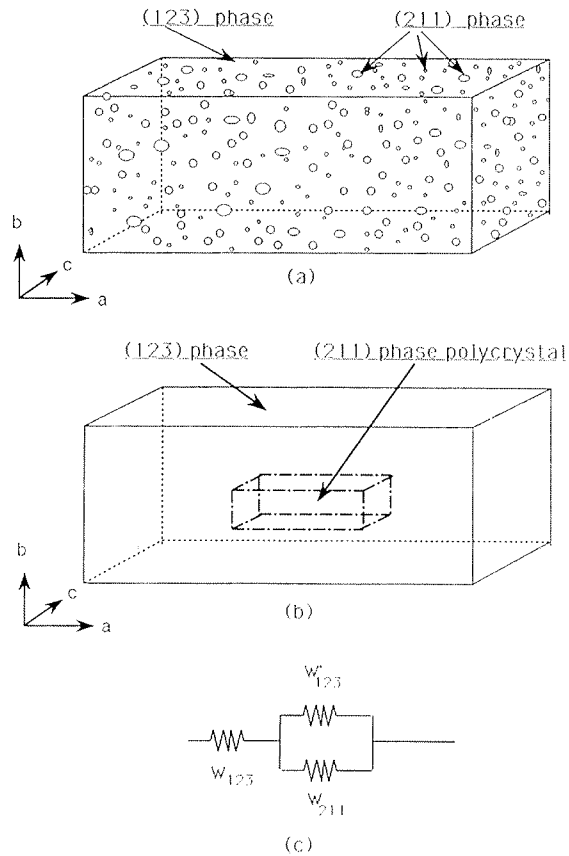

Figure 5 Schematic presentation of present model: (a) mixed crystal in which (211) phase particles are finely dispersed; (b) model structure to estimate thermal resistance *W*; (c) equivalent circuit to calculate *W*

flux is partly transported through the (211) phase particles. The contribution of an impurity particle to the thermal path does not depend on the position of the particle. Hence we can, theoretically speaking, concentrate all the (211) particles into a rectangular parallelepiped embedded in a (123) crystal, as shown in *Figure 5b*, and we can approximate the contribution of the (211) particles to the heat path from the parallelepiped (211) polycrystals.

Because the ideal densities of Y_2BaCuO_5 (6.22 g cm^{-3}) and $YBa_2Cu_3O_7$ (6.24 g cm^{-3}) are almost the same, the normal weight ratio can be regarded as the volume ratio of (211) and (123). So, if the sample size is $a \times b \times c$ and the (211) ratio is x, the size of the (211) rectangular parallelepiped is assumed to be $\sqrt[3]{x}a \times \sqrt[3]{x}b \times \sqrt[3]{x}c$.

In our model, the boundary scattering at the surfaces of the particles is replaced by the grain boundary scattering in the (211) polycrystal. Since metallographic observation of the present sample confirmed no anisotropy in the particle shape distribution, we assume that the grain boundary scattering in the (211) parallelepiped polycrystal is isotropic.

According to the model and with the heat flux along the a-direction in *Figure 5b*, the thermal resistance W of the specimen is given by the total resistance of the circuit schematically shown in *Figure 5c*

$$W = \frac{1}{\kappa}\frac{a}{bc} = W_{123} + \frac{W'_{123}W_{211}}{W'_{123} + W_{211}} \tag{1}$$

where W_{123}, W'_{123} and W_{211} are given by

$$W_{123} = \frac{1}{\kappa^{123}}\frac{a(1-x^{1/3})}{bc} \tag{2}$$

$$W'_{123} = \frac{1}{\kappa^{123}}\frac{ax^{1/3}}{bc(1-x^{2/3})} \tag{3}$$

$$W_{211} = \frac{1}{\kappa^{211}}\frac{ax^{1/3}}{bcx^{2/3}} \tag{4}$$

Using Equations (1)–(4), we can deduce the conductivity value κ^{123} of the $YBa_2Cu_3O_{7-X}$ component of the present mixed crystals if we know the thermal conductivity of the Y_2BaCuO_5 polycrystal κ^{211} and the (211) concentration x.

Figure 6 shows $\kappa^{211}(T)$ for the Y_2BaCuO_5 polycrystals sintered at temperatures between 950 and 1100°C. With decreasing measuring temperatures, $\kappa^{211}(T)$ slightly increased between 200 and 50 K and then decreased rather steeply below 50 K. The magnitude of κ^{211} of the polycrystals increased with increasing sintering temperatures. At the same time, the density of the polycrystal also increased from 3.0 g cm^{-3} at the sintering temperature of 950°C to 3.9 g cm^{-3} at 1100°C. On the other hand, the measured density of the MMTG mixed crystal was 5.9 g cm^{-3}.

Assuming that the thermal conductivity is roughly proportional to the density of the (211) specimen and the average density of the (211) particles in the mixed crystal is also 5.9 g cm^{-3}, the conductivity of the (211) sample sintered at 1100°C was multiplied by a factor of 1.51 (= 5.9/3.9) and the thus modified thermal conductivity *versus* T curve was used in the following analyses of $\kappa(T)$ for the mixed crystal.

Using $\kappa^{211}(T)$ and Equations (1)–(4), the conductivity

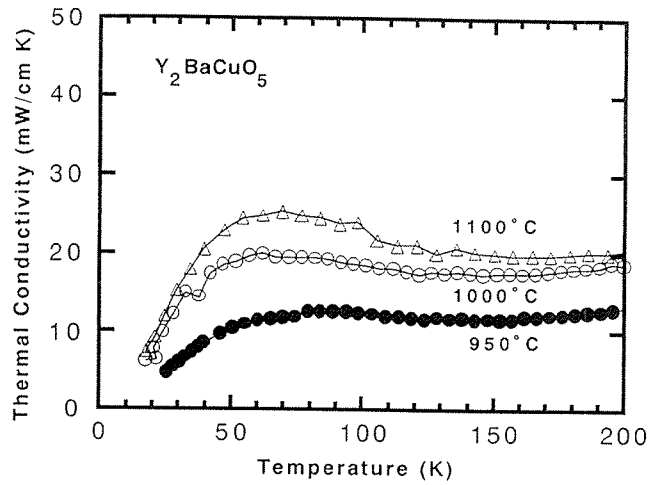

Figure 6 Thermal conductivity *versus* T of Y_2BaCuO_5 polycrystals sintered at various temperatures

of the (123) phase κ^{123} in the present MMTG mixed crystal was calculated. The calculated $\kappa^{123}_{ab}(T)$ values for S1 and S2 are shown in *Figures 7* and *8*, respectively. If the (211) phase particles do not contribute to the heat path of the mixed crystal ($\kappa^{211} = 0$), then Equation (1) reduces to

$$W^v = W_{123} + W'_{123} \tag{5}$$

Equation (5) corresponds to the case in which all the dispersed (211) particles in the mixed crystals are replaced by voids. Using the calculated κ^{123}, Equation (5) gives a somewhat smaller value for conductivity κ^v ($= 1/W^v$) than the observed value κ. The contribution of the (211) phase particles to the heat path in the a-b plane of the present mixed crystals can be estimated as the difference between κ_{ab} and κ^v_{ab}. $\kappa_{ab} - \kappa^v_{ab}$ is also shown in *Figures 7* and *8*.

Figures 7 and *8* suggest that κ^{123}_{ab} for S1 and S2 is fairly large and that the observed a-b plane conductivity κ_{ab} is appreciably reduced by the dispersed low conductive (211) particles. The ratio of κ_{ab} for S1 to S2 is 1.4, while the corresponding ratio of κ^{123}_{ab} is 1.55 at the maximum

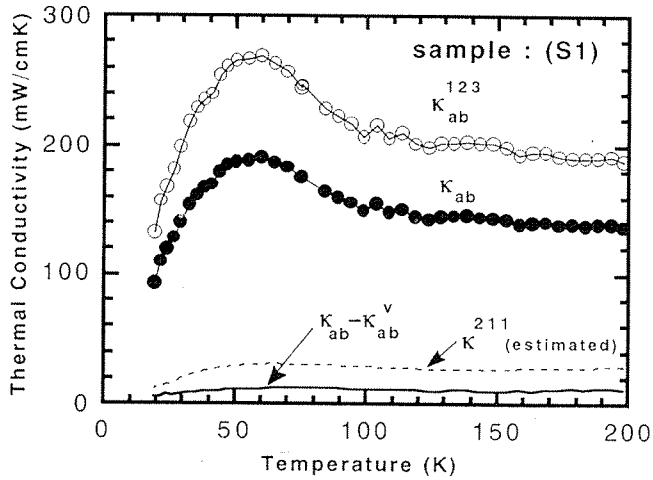

Figure 7 Calculated a-b plane thermal conductivity κ^{123}_{ab} *versus* T for $YBa_2Cu_3O_{7-X}$ matrix of S1 (○). Observed κ_{ab} for S1 is again shown for comparison (●). – – –, Estimated $\kappa^{211}(T)$ used for analyses; ——, $\kappa_{ab} - \kappa^v_{ab}$ (where $\kappa_{ab} - \kappa^v_{ab}$ stands for the contribution of dispersed (211) particles to heat path)

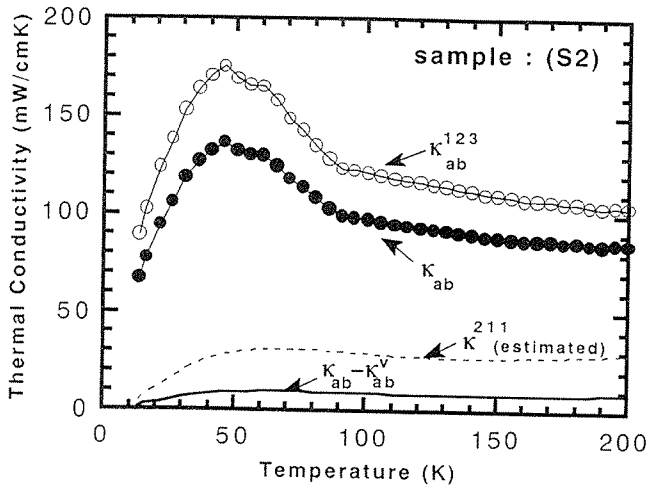

Figure 8 Calculated a-b plane thermal conductivity κ_{ab}^{123} *versus* T for $YBa_2Cu_3O_{7-X}$ matrix of S2. κ_{ab} of S2 is shown for comparison. ($\kappa_{ab} - \kappa_{ab}^{v}$ stands for the contribution of (211) particles to heat path)

point of conductivity. There seems to be an even larger difference in the conductivity of the (123) matrix between S1 and S2.

The small value of κ_{ab}^{123} for S2 again indicates that the $YBa_2Cu_3O_{7-X}$ matrix crystal in S2 is actually not as good as in S1. Sawano *et al.*[18] noted a tendency for the density of cracks to increase and J_c to decrease with decreasing (211) phase concentration. S2 contains a smaller amount of the (211) phase than S1. The measured J_c of S2 was actually as small as ≈ 100 A cm^{-2} at 77 K and was much smaller than the expected value of $\approx 10^4$ A cm^{-2} for good MMTG crystals. For use in practical applications, such as electrical power leads, it seems that MMTG crystals must be grown with a compositional ratio (123):(211) = 1:0.4.

Figure 9 shows the results of similar analyses for the c-axis conductivity κ_c. Since the observed κ_c is almost equal to the estimated κ^{211}, κ_c^{123} is almost equal to the observed conductivity. In the case of κ_c, (211) phase particles contribute to the heat path significantly. As a result, the upturn near T_c is somewhat enhanced in the estimated $\kappa_c^{123}(T)$. The anisotropy ratio $\kappa_{ab}^{123}/\kappa_c^{123}$ is

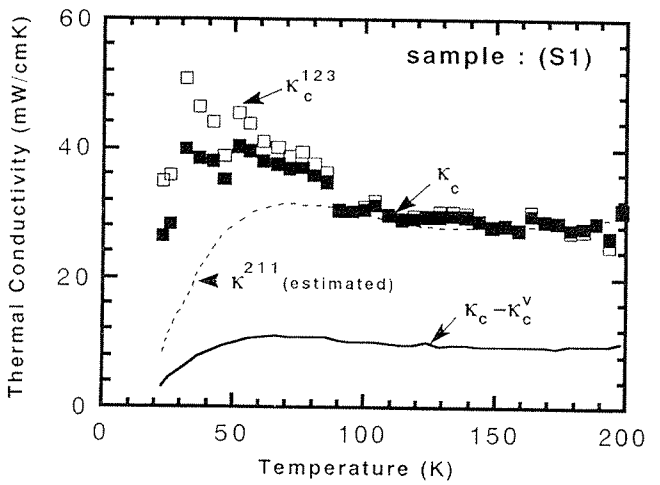

Figure 9 Calculated c-axis thermal conductivity κ_c^{123} *versus* T for $YBa_2Cu_3O_{7-X}$ matrix of S1 (□). Observed κ_c for S1 is again shown for comparison (■). – – –, Estimated $\kappa^{211}(T)$ used for analyses; ——, $\kappa_c - \kappa_c^{v}$ (where $\kappa_c - \kappa_c^{v}$ stands for the contribution of dispersed (211) particles to heat path)

≈ 6.3 and is enhanced compared with the observed value of $\kappa_{ab}/\kappa_c(\approx 5)$. Thus the anisotropy of the conductivity of the mixed crystal is reduced by the existence of dispersed (211) particles.

Summary

The thermal conductivity of $YBa_2Cu_3O_{7-X}$-Y_2BaCuO_5 mixed crystals prepared by modified melt texture growth was studied for two different composition ratios. A simple and elementary model was proposed to analyse the effect of finely dispersed Y_2BaCuO_5 particles on the thermal conductivity. The model allowed us to estimate the conductivity of the $YBa_2Cu_3O_{7-X}$ matrix. The observed a-b plane conductivity κ_{ab} is reduced by dispersed (211) phase particles in comparison with a pure (123) phase matrix.

In accord with results of the electrical resistivity measurements, the relatively high κ_{ab}^{123} values of the specimen with the composition ratio (123):(211) = 1:0.4 indicate better crystal growth conditions at this composition ratio. The observed c-axis thermal conductivity was hardly influenced by the (211) particles because the conductivity of the polycrystal Y_2BaCuO_5 and the c-axis conductivity of $YBa_2Cu_3O_{7-X}$ are of the same order. The observed anisotropy ratio κ_{ab}/κ_c is reduced in comparison with $\kappa_{ab}^{123}/\kappa_c^{123}$ for the $YBa_2Cu_3O_{7-X}$ matrix because of the existence of dispersed (211) particles.

Acknowledgement

The authors wish to thank Dr M. Matsukawa of Iwate University for valuable discussions.

References

1 **Murakami, M., Morita, M., Doi, K., Miyamoto, K.** *et al. Jpn J Appl Phys* (1988) **28** L399
2 **Jin, S., Tiefel, T.H., Sherwood, R.C., Dover, R.B.** *et al. Phys Rev B* (1988) **37** 7850
3 **Jezowski, A., Mucha, J., Rogachi, K., Horyn, R.** *et al. Phys Lett A* (1987) **122** 431
4 **Uher, C. and Kaiser, A.B.** *Phys Rev B* (1987) **36** 7135
5 **Morelli, D.T., Herremans, J. and Swets, D.E.** *Phys Rev B* (1987) **36** 3917
6 **Peacor, S.D., Cohn, J.L. and Uher, C.** *Phys Rev B* (1991) **43** 8721
7 **Hull, J.R.** *Cryogenics* (1989) **29** 1116
8 **Salama, K., Selvamanickam, V., Gao, L. and Sun, K.** *Appl Phys Lett* (1989) **54** 2352
9 **Yamamoto, H., Sato, M., Ozawa, S. and Tanaka, M.** *Supercond Sci Technol* (1991) **4** S355
10 **Kohayashi, S., Ishikawa, Y., Yoshizawa, S. and Kojima, H.** *Proc Int Superconducting Symposium (ISS) '92* Springer-Verlag, Tokyo, Japan (1993) 795
11 **Tenya, K., Miyajima, H., Ishikawa, Y., Kohayashi, S.** *et al. J Mag Sci Jpn* (1992) **16** 467
12 **Iye, Y., Tamegai, T., Sakakibara, T., Goto, T.** *et al. Physica C* (1989) **153/155** 26
13 **Friedmann, T.A., Rabin, M.W., Giapintzakis, J., Rice, J.P.** *et al. Phys. Rev. B* (1990) **42** 6217
14 **Hagen, J., Jing, T.W., Wang, Z.Z., Horvath, J.** *et al. Phys Rev B* (1988) **37** 7928
15 **Tozer, S.W., Kleinsasser, A.W., Penney, T., Kaiser, D.** *et al. Phys Rev Lett* (1987) **59** 1768
16 **Cohn, J.L., Wolf, S.A. and Vanderah, T.A.** *Phys Rev B* (1992) **45** 511
17 **Buravoi, S.E., Nefebov, K.V., Samoletov, V.A., Tallerczik, B.A.** *et al. Sov J Superconduct: Phys Chem Eng* (1989) **2** 32
18 **Sawano, K., Miura, M., Tanaka, M., Kimura, K.** *et al. Proc Int Superconducting Symposium (ISS) '90* Springer-Verlag, Tokyo, Japan (1991) 715